



Montes Bajo, M., Dunn, G., Stephen, A., Khalid, A., Cumming, D. R. S., Oxley, C. H., Glover, J., & Kuball, M. H. H. (2013). Impact ionisation electroluminescence in planar GaAs-based heterostructure Gunn diodes: Spatial distribution and impact of doping nonuniformities. *Journal of Applied Physics*, 113(12), [124505].  
<https://doi.org/10.1063/1.4798270>

Peer reviewed version

Link to published version (if available):  
[10.1063/1.4798270](https://doi.org/10.1063/1.4798270)

[Link to publication record in Explore Bristol Research](#)  
PDF-document

Copyright (2013) American Institute of Physics. This article may be downloaded for personal use only. Any other use requires prior permission of the author and the American Institute of Physics. The following article appeared in J. Appl. Phys. 113, 124505 (2013) and may be found at <http://link.aip.org/link/doi/10.1063/1.4798270>

## University of Bristol - Explore Bristol Research

### General rights

This document is made available in accordance with publisher policies. Please cite only the published version using the reference above. Full terms of use are available:  
<http://www.bristol.ac.uk/red/research-policy/pure/user-guides/ebr-terms/>

# Impact Ionisation Electroluminescence in Planar GaAs-based Heterostructure Gunn Diodes: Spatial Distribution and Impact of Doping Non-Uniformities

M. Montes Bajo<sup>1,\*</sup>, G. Dunn<sup>2</sup>, A. Stephen<sup>2</sup>, Ata Khalid<sup>3</sup>, D. R. S. Cumming<sup>3</sup>, C. H. Oxley<sup>4</sup>, J. Glover<sup>4</sup>, and M. Kuball<sup>1</sup>

<sup>1</sup>*Center for Device Thermography and Reliability, H. H. Wills Physics Laboratory, University of Bristol, BS8 1TL Bristol, U.K.*

<sup>2</sup>*Department of Physics, University of Aberdeen, King's College, AB24 3UE Aberdeen, U.K.*

<sup>3</sup>*School of Engineering, University of Glasgow, Rankine Building, G12 8LT Glasgow, U.K.*

<sup>4</sup>*Department of Engineering, DeMontfort University, The Gateway, LE1 9BH Leicester, U.K.*

## Abstract.

When biased in the negative differential resistance regime, electroluminescence (EL) is emitted from planar GaAs heterostructure Gunn diodes. This EL is due to the recombination of electrons in the device channel with holes that are generated by impact ionisation when the Gunn domains reach the anode edge. The EL forms non-uniform patterns whose intensity shows short-range intensity variations in the direction parallel to the contacts and decreases along the device channel towards the cathode. This paper employs Monte Carlo models, in conjunction with the experimental data, to analyse these non-uniform EL patterns and to study the carrier dynamics responsible for them. It is found that the short-range lateral (i.e. parallel to the device contacts) EL patterns are probably due to non-uniformities in the doping of the anode contact, illustrating the usefulness of EL analysis on the detection of such inhomogeneities. The overall decreasing EL intensity towards the anode is also discussed in terms of the interaction of holes with the time-dependent electric field due to the transit of the Gunn domains. Due to their lower relative mobility and the low electric field outside of the Gunn domain, freshly generated holes remain close to the anode until the arrival of a new domain accelerates them towards the cathode. When the average over the transit of several Gunn domains is considered, this results in a higher hole density, and hence a higher EL intensity, next to the anode.

---

\* Authors to which correspondence should be addressed: Miguel.Montes@bristol.ac.uk; Martin.Kuball@bristol.ac.uk

## 1.- Introduction

Planar high-electron-mobility-transistor (HEMT)-like Gunn diodes based on GaAs have recently been proposed as candidates for millimetre and THz range emission. This device design would potentially result in reduced heat generation and allow for improved heat extraction prospects when compared to the conventional vertical Gunn diode design<sup>1,2</sup>. Also, planar GaAs Gunn diodes would allow for an easier integration in monolithic microwave integrated circuits (as in Ref. 3) compared to their vertical Gunn diode counterparts. Fundamental mode operation at frequencies as high as 158 GHz have already been demonstrated from these devices<sup>4</sup>.

When planar GaAs Gunn diodes are biased in the negative differential resistance (NDR) regime, where Gunn oscillations start taking place, electroluminescence (EL) can be observed originating from the device channel. This indicates the presence of a significant impact ionisation primarily taking place when the travelling Gunn domains impinge on the anode contact edge, resulting in the generation of holes next to this contact<sup>5</sup>. The observed EL is not uniformly distributed over the device channel, but rather forms non-uniform patterns parallel to the anode whose intensity also varies along the device channel, being highest right next to the anode contact edge (Figure 1(a)). This is in contrast with previous observations of EL from other devices, such as GaAs-based HEMTs, in which impact ionisation is produced by the strong electric field at the drain-side-edge of the gate, resulting in the emission of light when the generated holes recombine with both hot electrons near the gate edge and cold electrons between the source and gate contacts.<sup>6,7,8,9</sup> Moreover, some of these reports indicate a higher EL intensity towards the source contact,<sup>7,9</sup> in contrast to observation on the planar Gunn devices considered in this work. Other devices, such as GaAs metal-semiconductor field-effect transistors (MESFETs)<sup>10</sup> show EL concentrated at the anode edge, also in contrast to the decreasing EL intensity towards the cathode contact characteristic to the heterostructure devices discussed here. In this paper, we illustrate, combining experimental results with Monte Carlo simulations, that EL emission can be used to analyse complex carrier dynamics,

and also to identify non-uniformities in doping concentration, such as those present in planar Gunn diodes, with the results applicable to a wider range of devices.

## **2.- Device structure and experimental procedure**

The devices studied in this work (Figure 1(b)) were grown by molecular beam epitaxy on semi-insulating GaAs substrates, and consist of an undoped 50 nm-thick GaAs channel surrounded by two 20 nm-thick  $\text{Al}_{0.2}\text{Ga}_{0.8}\text{As}$  barrier layers. Each of the barrier layers contains two evenly distributed  $\delta$ -doping layers doped with Si at an areal density of  $8 \times 10^{11} \text{ cm}^{-2}$ . This heterostructure yields an estimated electron density in the GaAs channel of  $\sim 10^{17} \text{ cm}^{-3}$ . The channel structure was covered by 15 nm of highly doped n-GaAs, on top of which multiple GaAs/InGaAs layers were grown to help in the formation of the ohmic contacts. These layers were subsequently etched away in the region between the electrodes during device processing, leaving the n-GaAs layer exposed. The active length of the devices was defined during fabrication by the deposition of the metallic ohmic electrodes and the devices were isolated by mesa chemical etching. More details on the growth and fabrication of these devices can be found elsewhere<sup>4</sup>. The Gunn devices were tested on-wafer and under DC bias at room temperature. Current through the device was continuously monitored to ensure no significant degradation of the device during the experiments. Maps of EL intensity on the device channel were obtained in dark conditions by collecting the emitted light through microscope using a 50 $\times$  objective lens with a numerical aperture of 0.50 and recording the light with an astronomy-grade near-infrared-sensitive charge-coupled device (CCD) camera. Spectrally resolved EL measurements were performed dispersing the collected light with a diffraction grating, then recording it with a Peltier-cooled CCD camera using a Renishaw InVia system.

## **3.- Experimental results**

### *3.1.- Spatial distribution of the electroluminescence*

EL features similar to those shown in Figure 1(a) were observed in all the studied devices when the applied bias was in the NDR regime. It must be noted that, in general, the EL intensity is not symmetrically distributed around the centre of the device.

The emitted light has its origin in the recombination of electrons and holes. The latter are generated by impact ionisation at the anode edge: the interaction of the Gunn domains with the high density of electrons underneath the anode contact edge results in electrons acquiring enough energy to generate holes by impact ionisation<sup>5</sup>. The EL spectrum (Figure 2(a)) shows a peak at the band gap energy of GaAs, indicating recombination of holes with cold electrons outside of the Gunn domain. Also, the spectrum features a high energy tail from which a typical equivalent electron temperature of  $\sim 1000$  K can be extracted, showing that impact-ionisation-generated holes also recombine with the hot electrons inside of the Gunn domain.<sup>5</sup>

Careful inspection of Figure 1(a) shows the EL intensity decreases towards the cathode contact with some modulations in the form of a series of brighter and darker vertical stripes parallel to the contact edges. These modulations and the overall decreasing trend of the EL intensity towards the cathode are also depicted in Figure 2(b). The higher EL intensity towards the anode indicates that, on average, there is a higher concentration of holes near the anode than near the cathode. On the other hand, Figure 2(c) illustrates the non-uniformity of the EL along the device width, i.e. parallel to the cathode and anode contacts. This is an indication that the generation of holes, and therefore impact ionisation is not occurring uniformly along the anode edge. Moving towards the cathode, some of the localised EL features of Figure 2(c) disappear, whereas others are visible up to the cathode edge. In none of these cases the EL features seem to spread laterally, indicating the impact ionisation generated holes do not spread significantly parallel to the contacts. Therefore, all these results indicate that, on average, the impact-ionisation-generated holes remain laterally localised at certain preferential locations, and spend more time near the anode.

In order to understand the carrier dynamics responsible for these EL features, Monte Carlo simulations of the transit of Gunn domains and the subsequent impact ionisation were

performed. A Keldysh model was used for the Monte Carlo simulations of the impact ionisation in the devices using bulk impact ionisation rates for the materials that form the device structure, as in Ref. 11. A series of devices ranging in channel length from 1 to 4  $\mu\text{m}$  was simulated, and it was found that current multiplication and impact ionisation occurred in the same way in all devices. Therefore, the Monte Carlo simulations shown in this work can be considered as representative of all the devices studied.

### *3.2.- Electroluminescence localisation parallel to the contacts: impact of doping non-uniformities*

Firstly the lateral localisation of the emitted light, i.e. the non-uniform intensity parallel to the contact edges, is discussed. A top-view two-dimensional representation of the Gunn diode three-dimensional structure was employed in which only one semiconductor material is involved and the ohmic contacts are represented by thin regions of higher doping at both ends of the channel (Figure 3).

In an ideal device, Gunn domains are expected to develop and travel towards the anode in a homogeneous fashion, i.e. as a charge plane wave. This is illustrated with a Monte Carlo simulation of such an ideal device in Figure 3(a). The simulated device is 1.4  $\mu\text{m}$  long and 7  $\mu\text{m}$  wide. This is smaller than the experimental devices shown in this work (typically 60  $\mu\text{m}$  wide and a few  $\mu\text{m}$  long) for computation reasons, but nevertheless still large enough to study EL localisation phenomena without being affected by border effects on the lateral edges of the channel. As the rate of impact ionisation in planar Gunn diodes depends only on the electric field and the electron charge density in the Gunn domains on the one hand, and the electron density underneath the anode edge on the other, holes are generated uniformly along the anode contact every time a Gunn domain reaches the anode edge<sup>5</sup>. This, however, does not reflect what is experimentally observed, i.e. EL non-uniformity.

The effect that a localised doping inhomogeneity in the anode contact would have on the domain formation, impact ionisation rate, and the dynamics of the thereby generated holes is considered in the following. Figure 3(b) shows the result of a simulation in which a small

perturbation in the form of a region of even higher electron concentration has been added to the anode contact. Such a doping perturbation could for example account for a non-uniform diffusion of ohmic contact metals upon alloying in this location. The introduced perturbation distorts the evolution of the Gunn domain, and due to the higher electron density in the perturbed region, the generation of holes by impact ionisation is higher at that region of the anode. The generated holes are attracted towards the cathode due to the applied electric field, and, although they spread laterally to some extent on their way to the cathode, they essentially remain laterally localised to a small region. This process repeats itself for each domain transit, which, for this simulation, lasts  $\sim 10$  ps.

To compare with the experimental results, the spatial distribution of the EL intensity is estimated using the product of electron and hole densities. As the EL experimental results are captured over times much longer than the transit times of the Gunn domains, we consider the electron-hole density product averaged over several Gunn domain transit periods (Figure 3(c)). It is apparent that there is a region of higher electron-hole product density in front of where the perturbation in the doping in the anode contact is. This is consistent with the experimental results, and demonstrates that EL can be used to detect small inhomogeneities in the charge density underneath the anode contact.

### *3.3.- Electroluminescence intensity from anode to cathode: interaction of holes with Gunn domains*

Figure 3(c) indicates the higher electron-hole product density region is located nearer to the anode than to the cathode, also consistent with Figures 1(a) and 2(b), and in contrast to what has been reported on Refs. 7 and 9. The top-view model employed in the previous section, however, is too simplistic to account for all the carrier dynamics characteristic of the heterostructure design of these devices. Therefore, two-dimensional lateral models were built, taking into account the actual layer structure of the devices as in Ref. 1, with the difference that in this work the high-charge-density region under the ohmic contacts only extended to the upper barrier of the channel.

It could be hypothesised that the EL observed at a distance from the anode edge is due to impact ionisation taking place as the Gunn domain travels along the channel in long devices, i.e. well before reaching the anode contact. So, it is worth verifying that, in the same way as has been previously reported for shorter devices,<sup>5</sup> impact ionisation also occurs primarily at the anode edge in the several  $\mu\text{m}$ -long devices studied here.

Figures 4(a), (b), and (c) show the simulated electric field during the transit of a Gunn domain in a 3  $\mu\text{m}$ -long device. The electric field inside of the domain first increases steadily as the domain progresses along the channel, and then increases strongly as the domain reaches the anode. Although the electric field inside of the domain reaches the threshold for impact ionisation in GaAs ( $\sim 200 \text{ kV/cm}^{11, 12, 13}$ ) before reaching the anode, it is not until that final moment that the electric field inside the Gunn domain is well above the threshold and therefore, the majority of impact ionisation events take place at the anode edge. To confirm this point, Figure 4(d) shows how the simulated impact ionisation events during the transit of a single domain occur primarily at the anode edge. This behaviour has been consistently observed in all the simulated devices, with lengths between 1 and 4  $\mu\text{m}$ .

According to this, the anode edge is the location of the highest electron and hole densities, and therefore the region where the EL intensity should be highest. Indeed, we have not observed any significant spread of the EL distribution towards the cathode as the bias is increased, supporting the conclusion that impact ionisation occurs primarily at the anode edge.

The impact-ionisation-generated holes remain close to the anode and only move slowly towards the cathode due to the combined effect of their relatively low diffusion coefficient<sup>12</sup> and the much lower electric field outside of the Gunn domain<sup>13</sup>. This is illustrated in Figure 5, which shows the electron and hole densities at several instants during the transit of a Gunn domain. Figure 5(a) shows a Gunn domain half way towards the anode whereas the holes generated by the previous Gunn domain are still close to the anode. When the Gunn domain reaches the anode edge and impact ionisation begins taking place, the holes that were still next to the anode are accelerated towards the cathode by the high electric field inside the



Gunn domain (Figure 5(b)). By the time the Gunn domain has almost left the device, and a new domain is already forming and starting its travel towards the anode (Figure 5(c)) there is a new collection of holes at the anode that, again, are subjected to a low electric field and only slowly move towards the cathode, and the cycle repeats again.

This indicates that, when averaged over several domain periods as in the experiment, there should be a locally enhanced density of holes near the anode, as holes spend more time in that region of the device. Indeed, if the electron and hole densities are averaged over several Gunn domain transits (see longitudinal density profiles of Figure 6(b), taken along the red line labelled *AB* of Figure 6(a)) it is found that the density of both charge carriers is higher next to and underneath the anode, then it reaches minimum a bit farther from the anode, and after that, it increases steadily towards the cathode. Also, the vertical density profiles of Figure 6(c) (taken along the blue line labelled *CD* in Figure 6(a)) indicate the band bending in the structure results in spatially separated electrons and holes, which would result in a low recombination rate allowing the holes to travel towards the cathode before recombining with electrons. This explains why EL is not concentrated at the anode edge in the devices under study, but rather decreases in intensity towards the cathode, in contrast to bulk GaAs planar Gunn devices (not shown) and previously reported MESFETs<sup>10</sup>.

To evaluate the results from the model, the electron-hole density product averaged over several Gunn domain transits is used as an estimation of the EL intensity, as above. The model predicts a higher EL intensity around the anode edge, a lower but still significant EL intensity in the rest of the channel, and finally another maximum in EL intensity next to the cathode (Figure 7(a)). Figure 7(b) shows a detail EL image from a comparable 2  $\mu\text{m}$ -long device. For clarity, Figure 7(c) shows the longitudinal (i.e. left to right in the figure) EL intensity profile obtained from Figure 7(b) at the location indicated by the arrows, and integrated vertically over a length indicated by the parallel lines. The EL intensity is maximum close to the anode, decreases towards the cathode, reaching a minimum roughly halfway between the contacts, and finally increases again reaching a local maximum closer to

the cathode edge. This is in good agreement with the Monte Carlo simulations of Figure 7(a) and confirms the validity of the model to explain the longitudinal localisation of holes next to the anode.

#### **4.- Conclusions**

We have demonstrated, with the aid of Monte Carlo simulations, that lateral non-uniform patterns formed by the impact ionisation-related EL in planar GaAs Gunn diodes illustrate local inhomogeneities on the doping of contacts, probably due to non-uniform intermixing of the metals during alloying. The decreasing EL intensity towards the cathode has been explained by the slow motion of impact ionisation generated holes due to their low relative mobility combined with the low electric field outside of the Gunn domain. Therefore, holes generated near the anode will only be accelerated when a new Gunn domain reaches them resulting on average in a peak of the electron-hole density product, and thus a higher EL intensity, near the anode contact. With all this, we have also proven that the combined use of EL analysis and Monte Carlo simulations is a very useful tool to analyse complex carrier dynamics in semiconductor devices.

#### **5.- Acknowledgements**

The authors acknowledge financial support from the Engineering and Physical Sciences Research Council (EPSRC) through EP/H011366/1, EP/H011862/1, EP/H012532/1 and EP/H012966/1.

## References.

- 
- <sup>1</sup> N. J. Pilgrim, A. Khalid, G. M. Dunn, and D. R. S. Cumming, *Semicond. Sci. Technol*, **23**, 075013 (2008)
- <sup>2</sup> A. Khalid, N. J. Pilgrim, G. M. Dunn, M. C. Holland, C. R. Stanley, I. G. Thayne, and D. R. S. Cumming, *IEEE Electron Device Lett.*, **28**, 849 (2007)
- <sup>3</sup> A. Förster, M. I. Lepsa, D. Freundt, J. Stock, and S. Montanari, *Appl. Phys. A*, **87**, 545 (2007)
- <sup>4</sup> C. Li, A. Khalid, N. Pilgrim, M. C. Holland, G. Dunn, and D. S. R. Cumming, *J. Phys. Conf. Ser.*, **193**, 012029 (2009)
- <sup>5</sup> M. Montes, G. Dunn, A. Stephen, Ata Khalid, C. Li, D. Cumming, C. H. Oxley, R. H. Hopper, and M. Kuball, *IEEE Trans. Electron Devices*, **59**, 654 (2012)
- <sup>6</sup> G. Meneghesso, T. Grave, M. Manfredi, M. Pavesi, C. Canali, and E. Zanoni, *IEEE Trans. Electron Devices*, **47**, 2 (2000)
- <sup>7</sup> N. Shigekawa, T. Enoki, T. Furuta, and H. Ito, *IEEE Electron Device Lett.*, **16**, 515 (1995)
- <sup>8</sup> M. Manfredi and M. Pavesi, *Phys. Status Solidi A-Appl. Mat.*, **201**, 1594 (2004)
- <sup>9</sup> A. A. Villanueva, J. A. del Alamo, T. Hisaka, K. Hayashi, and M. Somerville, *IEEE Trans. Device Mater. Reliab.*, **8**, 283 (2008)
- <sup>10</sup> H. P. Zappe and C. Moglestue, *J. Appl. Phys.*, **68**, 2501 (1990)
- <sup>11</sup> G. M. Dunn, G. J. Rees, J. P. R. David, S. A. Plimmary, and D. C. Herbertz, *Semicond. Sci. Technol.*, **12**, 111 (1997)
- <sup>12</sup> M. R. Brozel And C. E. Stillman, *Properties of Gallium Arsenide* (INSPEC, London, 1996), p. 89.
- <sup>13</sup> S. M. Sze and K. K. Ng, *Physics of Semiconductor Devices* (John Wiley & Sons, Inc, Hoboken, NJ, 2007), p. 517.

## Figures

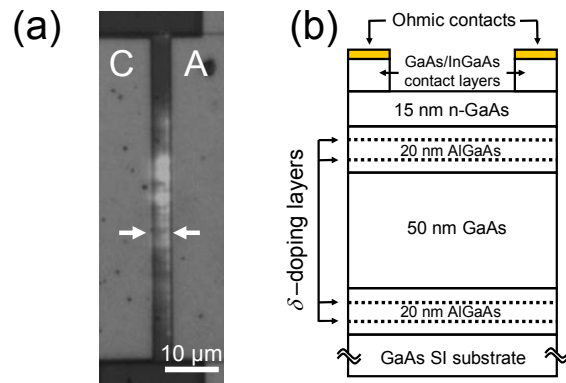


Figure 1. (a) Representative EL image from a 4  $\mu\text{m}$ -long and 60  $\mu\text{m}$ -wide Gunn diode biased at 8 V, overlaid on a white light image of the device. White arrows indicate the location from where the EL intensity profile of Figure 2(b) is extracted. (b) Schematic of the Gunn diodes analysed in this work.

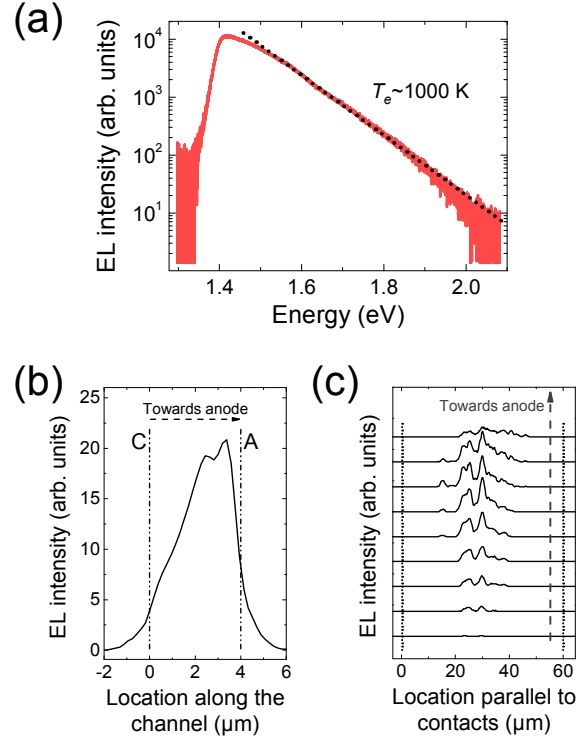


Figure 2. (a) Representative EL spectrum from a 2  $\mu\text{m}$ -long and 60  $\mu\text{m}$ -wide device biased at 4.5 V. The equivalent electron temperature is extracted from a fit to the high energy tail as indicated with the dotted line. (b) Longitudinal profile of EL intensity from Figure 1(a) along the line delimited by the white arrows. The vertical dash-dotted lines indicate the cathode and anode contacts. (c) EL intensity profiles obtained from the image in Figure 1(a) along lines parallel to the contacts, starting at the cathode edge, and in 0.5  $\mu\text{m}$  steps, offset for clarity. The two vertical dotted lines at the left and right sides of the figure indicate the lateral limits of the device mesa.

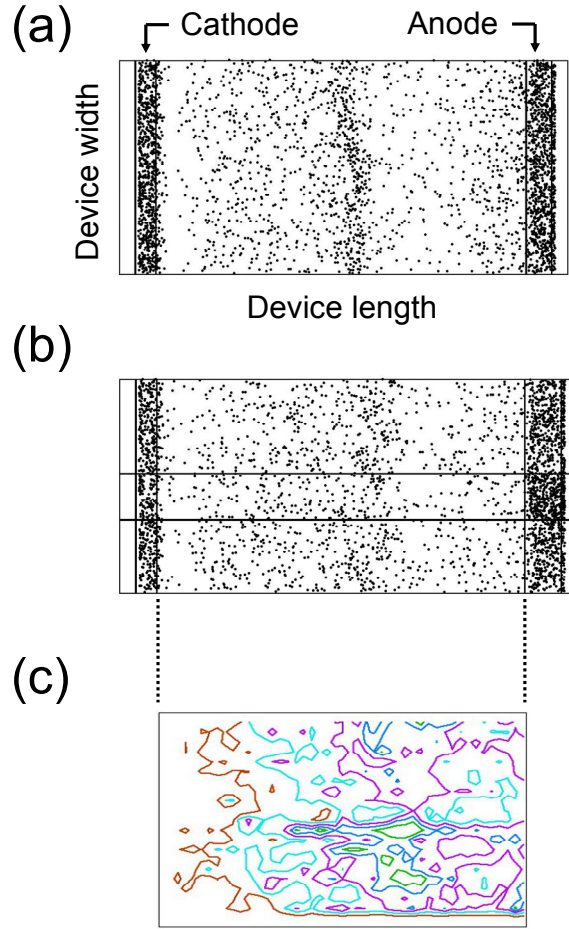


Figure 3. Top view Monte Carlo simulations of a planar Gunn device. (a) Evolution of the Gunn domains in a 7  $\mu\text{m}$ -wide and 1.4  $\mu\text{m}$ -long Gunn device biased at 6 V. Black dots, indicating electron particle positions, show a domain in transit. The two high electron density vertical stripes on the left and right ends are the cathode and anode ohmic contacts, respectively. Doping in the transit and contact regions was  $1 \times 10^{17}$  and  $1 \times 10^{18} \text{ cm}^{-3}$ , respectively. (b) Similar model as in (a) but with a higher electron density region ( $2 \times 10^{18} \text{ cm}^{-3}$ ) placed on the anode contact. The two parallel horizontal lines are a guide to the eye indicating the region of the device just in front of the doping inhomogeneity. (c) The density product of electrons and holes in the transit region, averaged over several Gunn domain transit periods, showing enhancement in the central region due to increased hole production in the higher density contact. Typical electron and hole densities are  $10^{17}$  and  $10^{16} \text{ cm}^{-3}$ , respectively. The step in electron-hole density product between consecutive contours is  $1 \times 10^{33} \text{ cm}^{-6}$ .

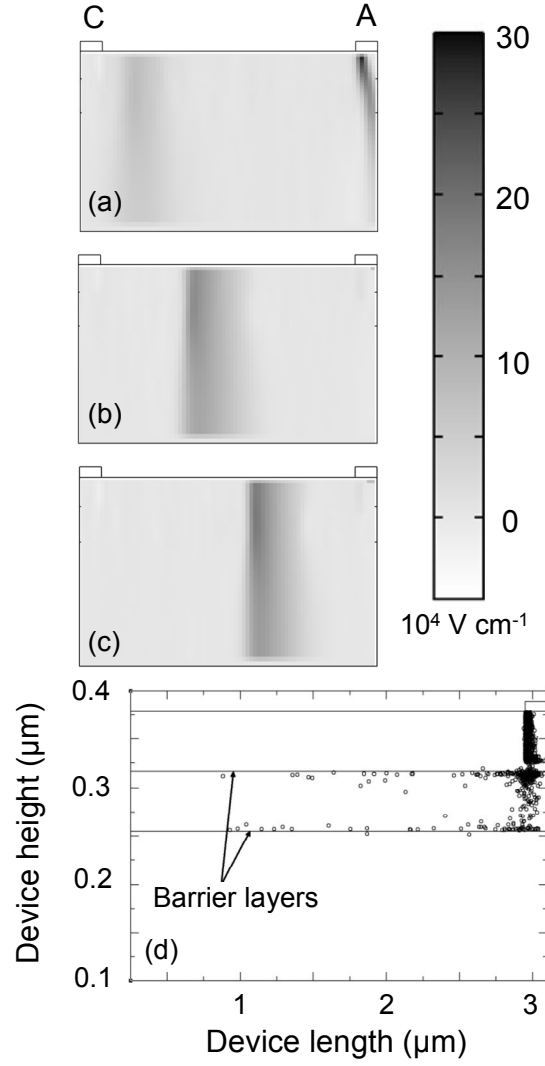


Figure 4. (a), (b), and (c), show the electric field in a 3  $\mu\text{m}$ -long device under 7 V bias at several instants during the transit of a Gunn domain. (a) One domain leaves the device, showing a maximum field of  $300 \text{ kV cm}^{-1}$ , whereas a new one forms at the cathode. (b) Same device 7 ps later, with the new domain progressing towards the anode. (c) After another 7 ps the domain has progressed further towards the anode and the field strength is becoming strong enough to cause some impact ionisation. (d) Impact ionisation event locations over the transit of a domain

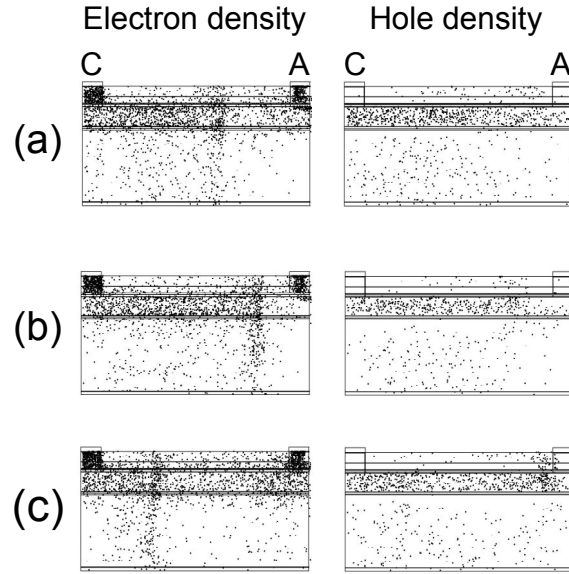


Figure 5. Electron (left column) and hole (right column) hole densities in a longitudinal section of a  $1.4\text{ }\mu\text{m}$ -long device operating at 6 V. (a) Domain about half way through the cycle with a high density of holes still under and close to the anode. (b) As the domain approaches the anode, the increasing field depletes the anode region of holes. (c) A newly forming domain with the old domain still passing out of the anode together with a new crop of holes next to the anode.



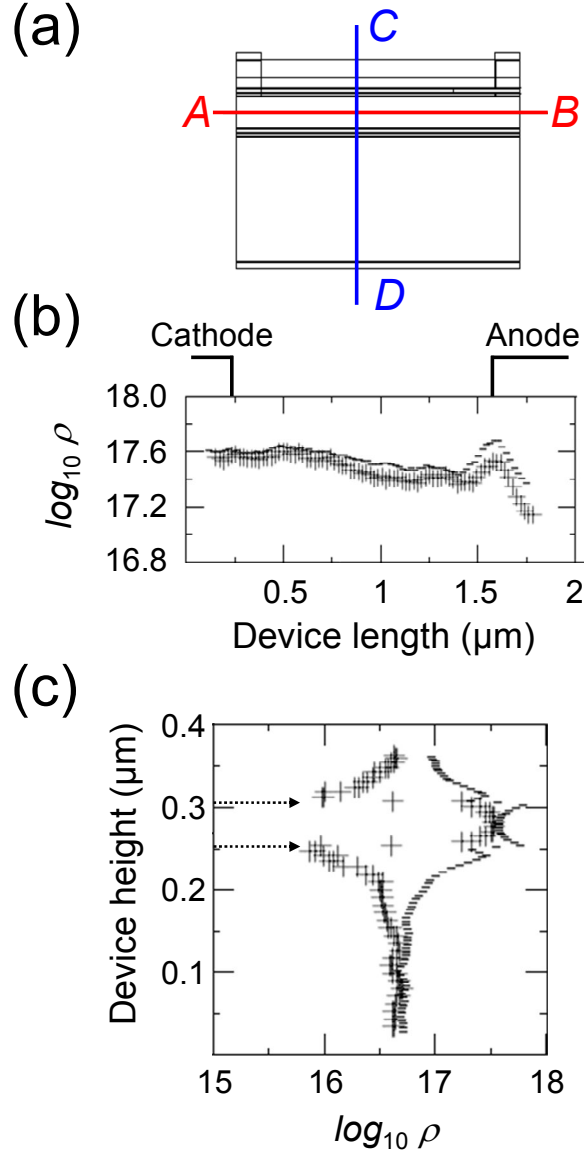


Figure 6. (a) Device schematic showing the lines along which the electron and hole density profiles of (b) and (c) are taken. (b) Electron (-) and hole (+) densities in the horizontal direction along the red  $AB$  line of (a). The location of the cathode and anode contact edges is indicated. (c) Electron (-) and hole (+) densities in the vertical direction along the blue  $CD$  line of (a). The dotted arrows indicate the location of the AlGaAs barrier layers. In (b) and (c), both the electron and hole densities are averaged over the transit of several Gunn domains and are shown as the  $\log_{10}$  of  $\rho$ , the density in  $\text{cm}^{-3}$ .

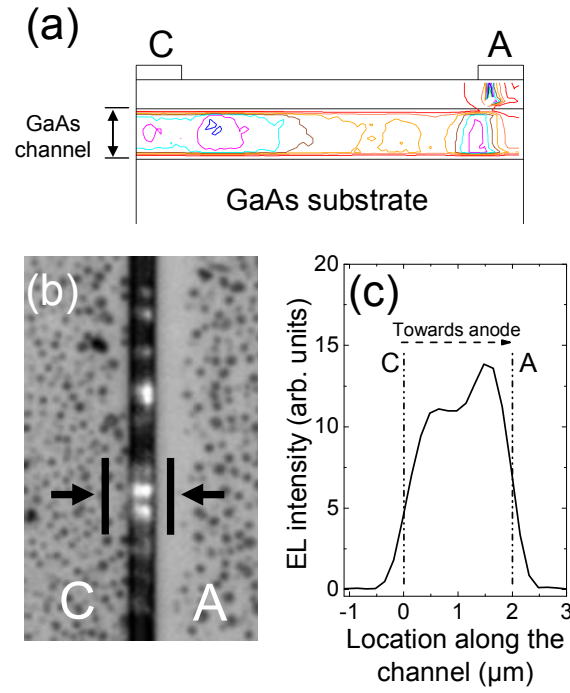


Figure 7. (a) Electron-hole density product in a longitudinal section of the device, averaged over the transit of several Gunn domains. The scale is the same as in Figure 3(c). (b) Detail of an EL image from a representative 2  $\mu\text{m}$ -long device biased at 6.5 V. (c) Longitudinal EL intensity profile from (b) at the location indicated by the arrows. The EL intensity at each point was integrated over the width indicated by the two parallel lines in (b). The vertical dashed lines indicate the location of the contact edges.